EVOLUTION OF INDARCH (EH4 CHONDRITE) AT 1 GPa AND HIGH TEMPERATURE.

S.Berthet [1, 2], V. Malavergne[1, 2], K.Righter[3]
[1]Lunar and Planetary Institute, Houston, TX 77058 U.S.A. and [2] Université Paris Est, Laboratoire des Géomatériaux et Géologie de l'Ingénieur (G2I), EA 4119, 5 boulevard Descartes, 77454 Marne-La-Vallée Cedex 2, France.
E-mail: berthet@lpi.usra.edu. [3]NASA Johnson Space Center, Houston, TX, U.S.A.

Introduction: The chondritic meteorites are materials that are as old as the solar system itself [1] characterized by variations in bulk chemical and oxidation state [2], and have long been considered possible building blocks that accreted to form the terrestrial inner planets. Enstatite chondrites contain nearly FeO-free enstatite, silicon-rich kamacite and various sulfides indicating formation under highly reducing conditions. These materials could have participated in the formation of the Earth [3,4].
However, "fingerprinting" of meteoritic materials has shown that no known meteoritic class corresponds to a hypothetical bulk Earth composition in every aspect [5]. To derive constraints on early accretion and differentiation processes and possibly resolve the debate on the formation of the Earth, it is required to study experimentally a variety of chondritic materials and investigate their melting relations and elemental partitioning behavior at variable pressure (P), temperature (T) and oxygen fugacities (f_{O2}). Variations in f_{O2} can indeed change chemical features and phase equilibria dramatically. The P-T phase diagrams of peridotites and carbonaceous chondrites have been extensively studied experimentally up to pressures and temperatures corresponding to the transition zone and lower mantle [e.g. 6,7,8]. Even though partial melting experiments have been conducted at ambient pressure on the enstatite chondrite Indarch [9], enstatite meteorites have never been experimentally investigated at high PT.

The following investigation focuses on the effect of the f_{O2} on the phase relations of Indarch, an EH4 chondrite.

Experimental and analytical methods: Piston-cylinder experiments were carried out at a pressure of 1 GPa and high temperature using the Lunar and Planetary Institute QuickPress at the NASA Johnson Space Center (Houston, Texas, USA). To vary the f_{O2} conditions, silicon metal was added to the starting material at different levels (0, 2, 4 and 6 wt%). Run products were investigated with a JEOL LV 5910 scanning electron microscope (equipped with an energy-dispersive X-ray analyzer), and a CAMECA SX-100 electron probe microanalyzer. For all run products, f_{O2}s were calculated using three different equilibria depending on the phases present in the samples [iron-wüstite (IW), iron-ferrosilite-fayalite (FeFsFa) and silicon-silicon oxide (Si-SiO_2)]. Then, they were all recalculated relative to the IW buffer.

Results and discussion: A total of 18 phase equilibria experiments were performed to constrain the evolution of the solidus and the liquidus of Indarch with oxygen fugacity at 1 GPa. The experimental conditions and results are summarized in Table 1. Oxygen fugacities relative to the IW buffer range from IW-1 to IW-5 depending on the level of Si at which the starting material was doped (Table 1). Under the P-T-fO_2 conditions of the experiments, the metallic phase was always liquid and quenched to two immiscible Fe-rich liquid alloys, one is S-poor and C-rich and the other one is S-rich and C-poor (Fig.1a.). The solubility of Si in the S-poor and C-rich FeNi alloy increases while the f_{O2} decreases.

With increasing temperature, for the three series of experiments at various oxygen fugacities, increasing degrees of silicate partial melting were observed (Table 1). At 1 GPa, the solidus temperature varies from below 1200°C at IW-1 to between 1300°C and 1400°C at around IW-5. The melting point is thus raised when highly reducing conditions, comparable to the ones prevailing during the formation of Indarch (IW-6, [9]), are reached. Similarly, the liquidus temperature varies from between 1550°C and 1600°C at IW-1 to between 1650°C and 1700°C at around IW-5. This is an increase in temperature in the range of 100°C.

Variable oxygen fugacity affected three aspects of the phase diagram. First, olivine is a stable phase at the most oxidized conditions. Second, grains of SiO_2 are observed for the samples doped with 4 and 6 wt% Si (Table 1) at all sub-liquidus T conditions. However, the study of the phase relations of the Indarch meteorite at ambient pressure [9] shows that, at IW-6, SiO_2 disappears above 1300°C. Moreover, no free-SiO_2 is observed for the run product #222 that was doped with only 2 wt% Si. Our observation suggests that we may have stabilized SiO_2 by adding more than 2 wt% Si to the starting material. And third, in the run products doped with 4 wt% Si and 6 wt% Si, i.e., a fO_2 between IW-4 and IW-5, grains of monosulfides (Mg, Mn, Fe)S were observed, in close association with grains of SiO_2 and FeNi alloys. However, none of these monosulfides were observed for the run products that were not doped with Si, i.e., fO_2 around IW -1. A study of the different mechanisms of formation of these phases [10] showed that it is indeed possible to crystallize (Mg,Fe)S through the following reaction:

$$2FeS+2MgSiO_{3_{silicate}}+Si_{metal} \leftrightarrow 2MgS+3SiO_2+2Fe$$

The solubility of S in the silicate melt depends strongly on the f_{O2} of the samples (Fig.2). This result is in agreement with the previous studies ([9], [10] and [11]).

Thus, this study of the evolution of the phase relations of an enstatite chondrite at 1 GPa with fO_2 supports the fact that the redox conditions are critical in determining a) the topology of the phase diagram at high temperatures, b) the stability of various phases (olivine, sulfide, silica), and c) the solubility of sulfur in the silicate melts. Clearly, oxygen fugacity has an important role during the formation and differentiation of planetary materials in the early solar system.

References: [1] Amelin Y. et al. (2002) *Science, 297,* 1678-1683. [2] Krot A.N. et al. (2003) *Treatise in Geochemistry,Vol.1,* 83-128.[3] Wänke H. and Dreibus G. (1988), *Phil.Trans.R.Soc.London, A 325,*545-557. [4] Javoy M. (1995) *GRL, 22,*2219-2222. [5] Drake M.J. and Righter K. (2002) *Nature, 416,*39-44. [6] Agee C.B. et al. (1995) *JGR, 100,* 17725-17740. [7] Asahara Y. et al. (2004) *PEPI, 143-144,* 421-432. [8] Tronnes R.G. and Frost D.J. (2002) *EPSL, 197,* 117-131. [9] McCoy T.J. et al. (1999) *MAPS, 34,* 735-746. [10] Malavergne et al. (2007) *LPSC XXXVIII,* Abstract # 1737. [11] Holzheid et al. (2002) *Am.Min., 87,* 227-237.

Run #	Si added (wt%)	T (°C)	Duration	ΔIW	Phase assembly	Proportion of silicate melt (%)
220	0	1200	42h15min	-1.2	px, ol, sm, mm	7
173	0	1300	8h25min	-1.4	px, ol, sm, mm	10
206	0	1500	4 h	-1.2	px, ol, sm, mm	40
192	0	1550	1h 30min	-1.3	px, ol, sm, mm	55
175	0	1600	1h 20min	-1.6	sm, mm	100
153	0	1700	70 min	-1.7	sm, mm	100
222	2	1600	1h30min	-2.8	px, sm, mm	34
211	4	1300	17h20min	-4.6	px, SiO_2, mm	0
316	4	1400	24h25min	-4.0	px, SiO_2, sm, mm, ms	17
239	4	1500	3h30min	-4.0	px, SiO_2, sm, mm, ms	29
314	4	1600	1h30min	-4.0	px, SiO_2, sm, mm, ms	35
212	4	1700	1h	-3.9	sm, mm	100
207	6	1300	16h35min	-5.2	px, SiO_2, mm	0
315	6	1400	24h	-5.0	px, SiO_2, sm, mm, ms	16
171	6	1500	2 h	-4.9	px, SiO_2, sm, mm, ms	25
313	6	1600	1h30min	-4.2	px, SiO_2, sm, mm, ms	34
240	6	1650	1h 05min	-4.0	px, SiO_2, sm, mm, ms	40
179	6	1700	1 h	-4.3	sm, mm	100

Table 1. Experimental conditions and results. All experiments were performed at 1 GPa. sm, silicate melt; mm, metallic melt; px, pyroxene; ol, olivine; ms, monosulfides.

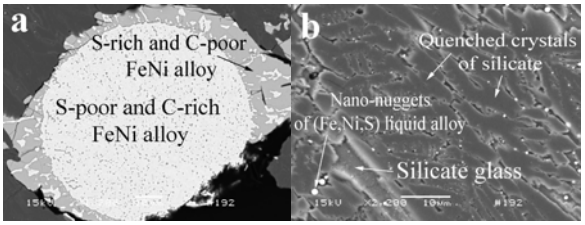

Fig.1. a. Backscattered electron (BSE) image of the typical metallic phase present in all run products (e.g., #192-no Si added-1GPa-1550°C). The metallic phase quenched to two immiscible liquids: a core of S-poor and C-rich FeNi alloy is surrounded by a quenched texture: the bright phase has a composition close to the one of the core and the dark phase that represents most of the ring is S-rich and C-poor FeNi alloy. The two immiscible liquids are in equilibrium with each other and with the silicate liquid. **b.** BSE image of the silicate liquid phase in sample #192. Nano-nuggets of metallic (Fe,Ni,S) alloy are disseminated in the silicate liquid phase, which did not quench to a glass but recrystallized to give this structure of quenched crystals.

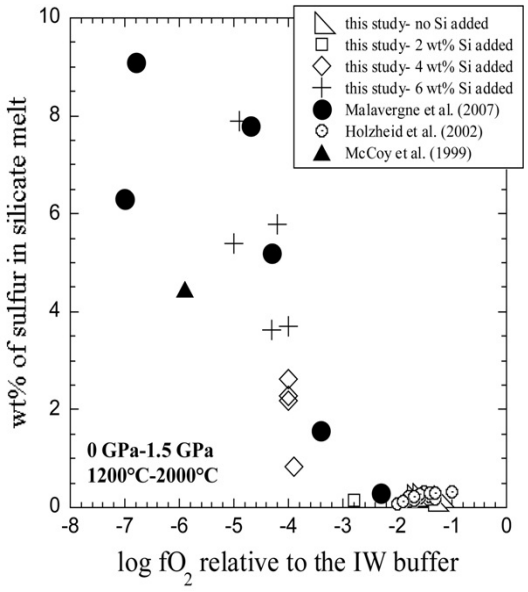

Fig.2. Sulfur content (in wt%) in the silicate melt as a function of oxygen fugacity. 2σ–errors are generally within the size of the symbols. Note that the plotted data of this study, and previous studies ([9], [10] and [11]), span a range of different P and T conditions.